



ELSEVIER

Thermochimica Acta 262 (1995) 55–68

thermochimica
acta

A novel isothermal electrochemical microcalorimeter

Robin J.H. Clark *, Yongchun Zhu

Christopher Ingold Laboratories, University College London, 20 Gordon Street, London WC1H 0AJ, UK

Received 5 December 1994; accepted 10 February 1995

Abstract

A novel isothermal electrochemical microcalorimeter has been designed and tested. It shows a very fast response to temperature change at the working electrode surface, and can be used to monitor the cyclic voltammetric programme, the optimum sweep rate being 0.020 V s^{-1} . The cyclic voltammetric thermogram can be used to estimate the enthalpy change of an electrochemical reaction. A sensitivity factor of $3.012 \times 10^{-5} \text{ J mV}^{-1}$ is derived for the response of the Wheatstone bridge to the enthalpy change in a chemical reaction via the instantaneous measurement of temperature change at the working electrode surface. A one-dimensional semi-infinite diffusion model has been adopted and numerically simulated to describe qualitatively of the response function of the measuring system to the sweep rate in a cyclic voltammetric programme. A lock-in amplifier has been used in the Wheatstone bridge electric circuit and offers a high quality of amplification for a weak electric signal.

Keywords: Cyclic voltammetric thermogram; Isothermal electrochemical microcalorimeter

1. Introduction

Calorimetric and thermometric techniques are important methods of investigation in many branches of pure and applied chemistry [1–3] and biology [4]. Some papers on electrochemical calorimetry have been published concerning gas evolution and “cold fusion” [5–7], metal surface corrosion [1], electrochemical reactions [8, 9], and adsorption [10]. There are some differences between electrochemical calorimetry and normal calorimetry. Firstly, the reactions are induced at electrodes and controlled by

* Corresponding author.

electrochemical methods without solution mixing problems; secondly, the reactions occur at the electrode surface, not in the bulk solution, and so the diffusion of heat is the major problem in the measurement; thirdly, compared with that in bulk solution, the reaction rate is very low, and the amount of reactant taking part in an electrochemical reaction is very small, so that the enthalpy of reaction and the temperature change at the electrode surface are very small. Therefore, instantaneous measurement is preferable. Introduction of electrodes into, and the passage of electricity through, the calorimeter can also result in some problems which make the measurements difficult, i.e. those associated with knowing the adsorption enthalpies of reactants and products, the Peltier effect of the solution, and the ohmic effect. It is necessary to design and build a fast-response, high-sensitivity microcalorimeter for electrochemical use. It is also necessary to find out and evaluate the response function of the calorimeter so that the experimental conditions of calorimetry–electrochemistry can be optimized. In the present paper, a suitable microcalorimeter has been designed and tested and a numerical simulation method has been used to explain the response function of the electrochemical calorimeter to the sweep rate in cyclic voltammetry.

2. Design of a microcalorimeter and its measurement system

In order to get a fast response to a temperature change, a 10 k Ω (25°C) bead-shaped RT curve-matched thermistor with a negative temperature coefficient was used as a temperature probe. The working thermistor is attached to the inner surface of a platinum slice (0.1 mm thick) at the bottom of a Teflon support bar. The outside of the platinum slice makes contact with the sample solution. In this case the platinum slice has two functions: the outside surface is a working electrode and the inside surface, in contact with a working thermistor, is a heat conducting medium. The heat produced at the electrode surface must diffuse through the platinum slice first, so that the thermistor can instantaneously monitor the temperature change of the electrode surface during an electrochemical process, as shown in Fig. 1(f). Note that the thermal diffusivities of platinum, aqueous solution, Teflon, and air are 0.274, 0.00136, 0.00109 and 0.222 cm² s⁻¹, respectively.

An isothermal cell was made with a cell support of a Teflon bar (5 cm in diameter and 10 cm in length), which has good insulation properties for heat and electricity, and is inert to chemicals. A Ag/AgCl reference electrode, a spiral platinum wire auxiliary electrode, a Pt-slice working electrode with working thermistor, a reference thermistor (the same as the working thermistor), which is put into a glass tube with a platinum wire sintered at its top end as a heat-conducting medium, and a mercury thermometer to read the temperature of the appropriate sample solution were put into the cell in their own chambers, which were connected to each other via a small channel about 2 mm in diameter as shown in Fig. 1. During experiments, all parts were fixed into their chambers with Teflon tape and the entire isothermal cell was placed in a 500 cm³ thermostatted water bath to minimize the effects of fluctuations in room temperature. The size of the cavity for the sample solution could be adjusted by altering the

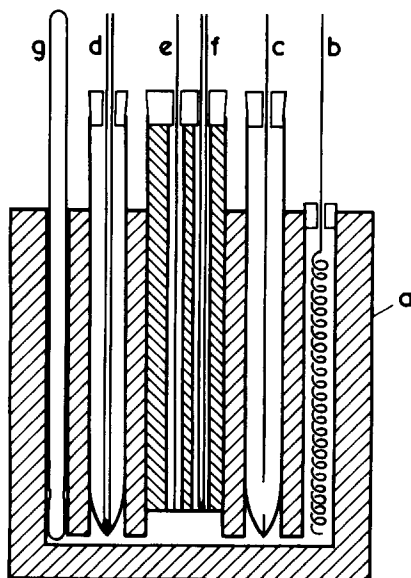


Fig. 1. Isothermal electrochemical microcalorimeter cell: a, teflon support; b, auxiliary electrode; c, Ag/AgCl reference electrode; d, reference thermistor; e, working electrode; f, working thermistor; g, thermometer.

depth of the support bar of the working electrode. In this way the cell can also serve as a thin-layer electrochemical cell.

The temperature change was measured by two thermistors which formed two arms of a Wheatstone bridge and thus formed a differential temperature measuring system. The Wheatstone bridge was powered by a 1.34 V mercury battery and gave out a stable signal with an acceptable noise level. The signal from the bridge was very small, so a lock-in amplifier was used to increase the signal by up to 100 times so that it could be monitored easily by a multimeter or computer. The electric circuit is shown in Fig. 2.

In the experiments, a digital multimeter with ± 0.001 mV reading error, and a model 28000 x - y recorder (Bryans Southern Instruments) were used to monitor and record the signal. All leads were shielded coaxial cables. All parts of the measuring system were covered by metal boxes with a common earth wire so that all sources of electrical noise were reduced as far as possible.

3. Evaluation of the microcalorimeter

3.1. Electrical tests

The temperature change in a resistive element on passage of electric current is proportional to the power and time. When a thermistor in a Wheatstone bridge is used

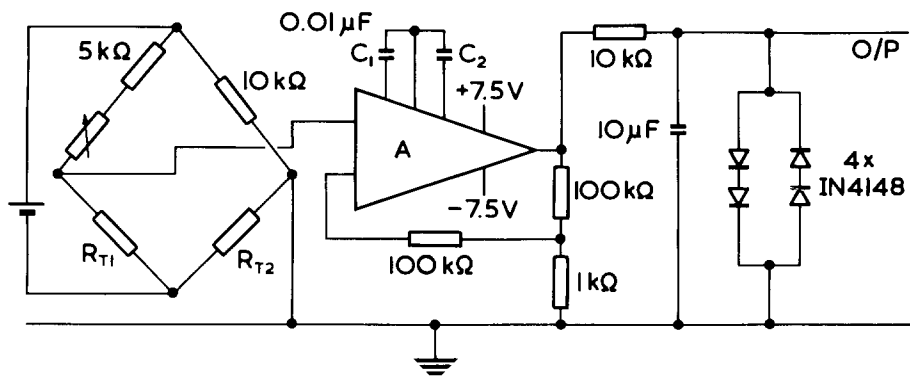


Fig. 2. Electric circuit of the temperature measuring system. R_{T1} , R_{T2} are RT curve-matched thermistors (NTC, 10 k Ω at 25°C); A: ICL 7605.

to monitor the temperature change, the output of the Wheatstone bridge, E_{OB}/mV , follows the equation

$$E_{OB} = btE^2/R \quad (1)$$

where b is a proportionality constant, E/V is the potential applied to the resistive element, and R/Ω is the resistance, and t is the time. Eq. (1) has been used to calibrate a calorimeter [11].

A 100.5 Ω (0.25 W) resistor was fixed to the surface of the platinum working electrode and sealed into a 2 cm diameter glass tube. The latter was then placed into a 50 cm³ beaker filled with water, and thermostatted at 18.2°C. A steady baseline signal (E_{OB} vs. t) was obtained before a potential was applied to the resistor; a steady baseline was obtained after ~ 100 s on average. The baseline has 0.08 mV noise (2.5 mV scale), which equals $\pm 0.8 \mu V$ before amplification.

A 1.000 V potential from a millivolt source (Time Electronics Ltd., model 404 S) was applied to the 100.5 Ω resistor while the output of the Wheatstone bridge, E_{OB}/V , was monitored as a function of time (Fig. 3(1)). This procedure was repeated for a 1010 Ω resistor with applied potentials of 1.000 and 0.500 V (Fig. 3(2) and 3(3)). The experiments show that the thermistor responds linearly to temperature change, as measured by the output of the Wheatstone bridge from 0 to 100 mV. The measurement of the reaction enthalpy did not require an exact knowledge of the potential-against-temperature conversion factor, but the potential-against-enthalpy conversion factor is necessary and is defined as the sensitivity factor (b), obtained from the slope of each line in Fig. 3. The reciprocal of b , $1/b$, is the sensitivity factor of the output of the Wheatstone bridge, E_{OB}/mV , to electric power released to the isothermal cell. Under the experimental conditions described, $1/b_1 = 9.95 \times 10^{-4} \text{ W s mV}^{-1}$, $1/b_2 = 7.27 \times 10^{-4} \text{ W s mV}^{-1}$, $1/b_3 = 7.35 \times 10^{-4} \text{ W s mV}^{-1}$, which show that different resistor as heat sources have different sensitivity factors; for the same resistor with different applied potentials, the sensitivity factors are not changed. From these results

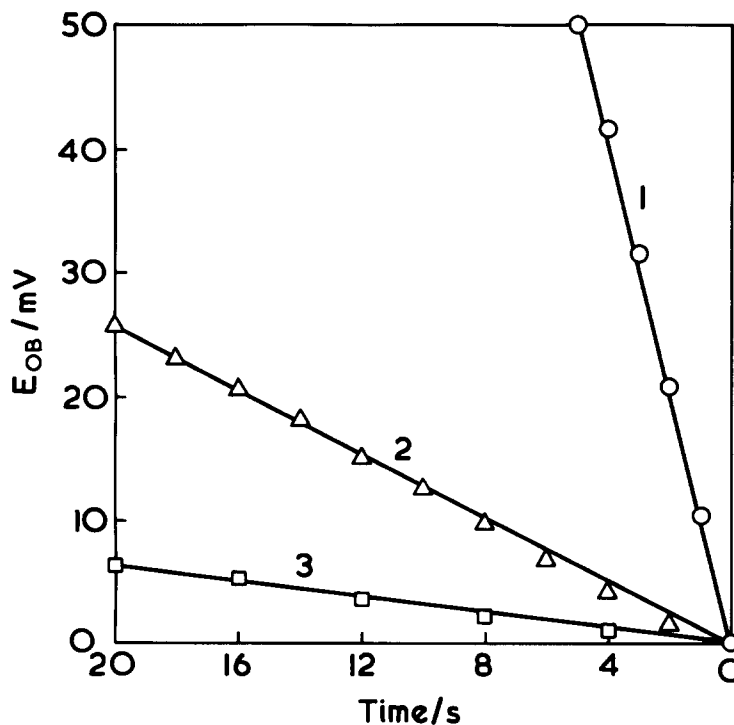


Fig. 3. Calibration lines: 1, 100.5 Ω , 1.000 V; 2, 1010 Ω , 1.000 V; 3, 1010 Ω , 0.500 V.

we can see that temperature change is linearly related to the voltage change. However, it does not represent the real situation in which the platinum electrode makes contact with aqueous solution rather than air; moreover, chemical or electrochemical reaction heating (or cooling) sources are different from the heat generated by an electrical resistance for a given amount of applied potential, and would give rise to different sensitivity factors for the response curve of the isothermal calorimeter.

3.2. Chemical test

The endothermic enthalpy of mixing of tri-(hydroxymethyl)-aminomethane (TRIS) with a dilute solution of sodium hydroxide has been shown to be a suitable standard for solution calorimetry [12, 13]. The enthalpy of this reaction is dependent on the concentration of base and has been shown to follow the equation

$$\Delta H/\text{J mol}^{-1} = 17690 - 10636(c_{\text{NaOH}}^0/\text{mol dm}^{-3}) + 5233.1(c_{\text{NaOH}}^0/\text{mol dm}^{-3})^2 \quad (2)$$

in which c_{NaOH}^0 is the concentration of NaOH. This reaction has been used to test our microcalorimeter. Analytically pure TRIS was prepared at a concentration of 0.200 mol dm⁻³. Sodium hydroxide, analytically pure, was prepared at 0.01 mol dm⁻³

and diluted to $9.38 \times 10^{-4} \text{ mol dm}^{-3}$ before use. The enthalpy of reaction was calculated from Eq. (2) to be $17.68 \text{ kJ mol}^{-1}$. A low concentration of NaOH was used to imitate the real voltammetric experiment in which there is only a very small temperature change. The aqueous solution of NaOH was injected into the isothermal cell via a carefully positioned capillary, so as to introduce the base solution as close as possible to the surface of the working electrode, thus simulating an electrochemical reaction at the electrode. A typical signal change, E_{OB} , is shown in Fig. 4. By adding different volumes, V_{NaOH} , of NaOH solution to the cell, a calibration line was obtained, which followed the equation $E_{OB}/\text{mV} = 0.462 - 550.6 V_{\text{NaOH}}/\text{cm}^3$, with a correlation coefficient $r = 1.023$, and a maximum relative standard deviation of 3.7% for each experimental point. Calculating from the slope of the linear equation, the concentration of NaOH, and the enthalpy of the reaction, the sensitivity factor of the system was found to be $3.012 \times 10^{-5} \text{ J mV}^{-1}$ (compare with the sensitivity factor found for the electrical tests in 3.1).

3.3. Electrochemical tests

$\text{K}_3[\text{Fe}(\text{CN})_6]$ was chosen to evaluate the electrochemical microcalorimeter and its response to an electrochemical reaction.

A model 174A PAR, 7040A x - y recorder and a Metrohm E612 VA scanner were included in the electrochemical system. The isothermal cell was first filled with 0.50 mol dm^{-3} KCl aqueous solution and put into a 500 cm^3 beaker with water. After equilibration of the system cyclic voltammetry was performed and a good base cyclic voltammogram was recorded, but no heat was released or absorbed during the process. Then the ferricyanide system was studied by the same procedure. A 0.60 V potential, to which the system had no response, was applied to the system first. After that, cyclic

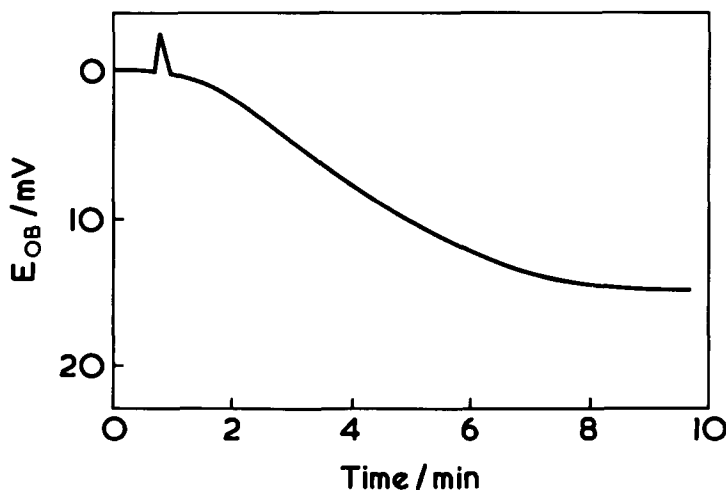


Fig. 4. The signal change after injection of NaOH solution: $c_{\text{NaOH}}^0 = 0.000938 \text{ mol dm}^{-3}$; $V_{\text{NaOH}} = 0.030 \text{ cm}^3$.

voltammetry was performed, and a cyclic voltammogram and a cyclic voltammetric thermogram were recorded at the same time (Fig. 5a). A current–time curve was obtained as shown in Fig. 5b. Numerically differentiating the cyclic voltammetric thermogram (CVT) with time, a cyclic voltammetric differential thermogram (CVDT) was obtained as shown in Fig. 5c. Comparing the current–time, CVT and CVDT curves in Fig. 5, we can see that current–time and CVDT curves have peaks at the same time or at the same potential, which means that the CVDT has similar properties to the CV and can be used to study the mechanism of an electrochemical reaction; the CVT curve shows integrated properties, from which the enthalpy of an electrochemical reaction can be estimated because the influence of the heat source via the auxiliary electrode can be omitted on the experimental time scale, and ohmic heating can also be neglected for a large enthalpy change associated with an electrochemical reaction ($> 100 \text{ kJ mol}^{-1}$). For the ferricyanide system, the measured enthalpy of the electrochemical reaction was $-356.1 \text{ kJ mol}^{-1}$ ($-358.4 \text{ kJ mol}^{-1}$ from thermodynamic data) as has been described elsewhere [14].

From the experimental results we found that different sweep rates gave out different signals responding to the temperature change under the same experimental conditions. At the same sweep rate, the signals were the same, with the maximum relative deviation being 2.3% for five measurements at each experimental point. Plotting the maximum of the signals, E_{OB}/mV , against sweep rate, the response curve of the electrochemical microcalorimeter to the sweep rate of the potential scan was obtained as shown in Fig. 6. This curve is divided into two parts with a cross-over point at the sweep rate of 0.02 V s^{-1} , which is the optimum. By plotting the logarithm of the maximum of the signal in the CVT for each sweep rate, $\ln(E_{OB}/\text{mV})$, against the sweep rate, $v/\text{V s}^{-1}$, two straight lines were obtained. One of these, $y = 0.2280 + 0.1655x$ with $r = 0.9813$ and sum of squared deviation (SSD) = 4.719×10^{-6} , is for the first part of the curve. The other, $y = -0.2309 - 0.1708x$, with $r = 0.9975$ and SSD = 1.4349×10^{-5} , is for the second part of the curve.

4. Mathematical model and numerical simulations of the system

An isothermal cell with a plane electrode can be used to study one-dimensional semi-infinite heat conduction in a heterogeneous medium, as shown in Fig. 7.

There are two holes (2.5 mm in diameter) for the electrode and working thermistor leads in the Teflon bar. The air in the holes is in contact with the inside surface of the platinum slice. Since the thermal diffusivity of Teflon in contact with the platinum slice is very small ($0.00109 \text{ cm}^2 \text{ s}^{-1}$) and can be neglected compared with that of air ($0.222 \text{ cm}^2 \text{ s}^{-1}$), we consider that a 0.01 cm thick Pt slice is in contact with a 0.05 cm thick layer of aqueous solution on one side, and with a 0.04 cm section of air on the other side. The left end of the air layer is the zero point of the x axis. The working thermistor is put at point A on the air side of the platinum slice with temperature $T(l, t)$; the other side of the Pt slice is the working electrode surface with temperature $T(g, t)$. The reference thermistor is put at B with temperature T_r , which is far from that of the measuring system; it is assumed that T_r is not changed during the experiments.

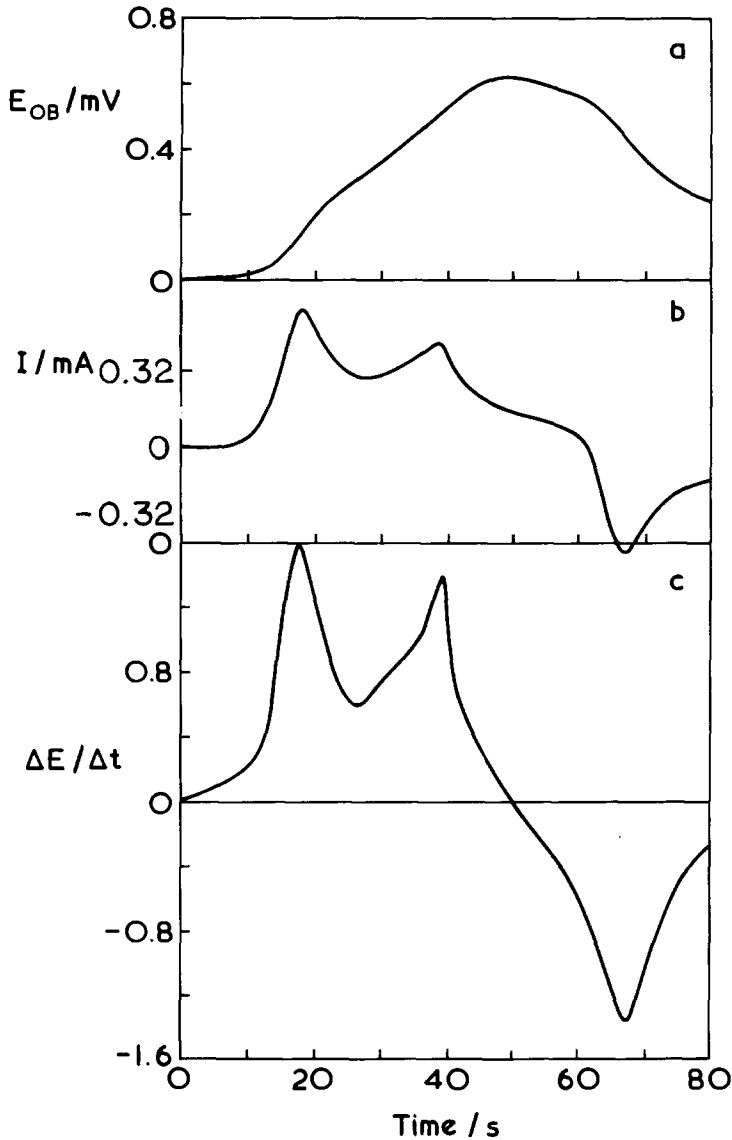


Fig. 5. (a) Cyclic voltammetric thermogram (CVT); (b) current–time curve of a CV; (c) cyclic voltammetric differential thermogram (CVDT). The concentration of $K_3[Fe(CN)_6]$, $c^0 = 2.00 \times 10^{-3} \text{ mol dm}^{-3}$ in 0.50 mol dm^{-3} KCl aqueous solution (pH 6.0); sweep rate, 0.020 V s^{-1} . The second peak at $\sim 40 \text{ s}$ will be discussed elsewhere [14a].

4.1. Temperature distribution with time for a given $T(g, t)$

In the heterogeneous medium described in Fig. 7, both sides of the electrode surface were considered to be homogeneous media and divided into 5 regions. From left to

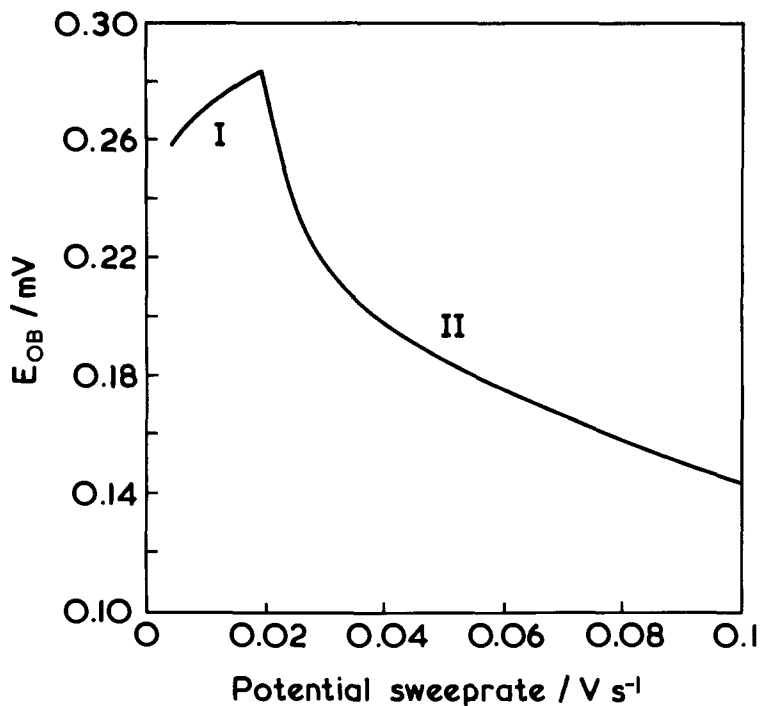


Fig. 6. Response function of electrochemical microcalorimeter to the sweep rate of the cyclic voltammogram. The experimental conditions were the same as in Fig. 5.

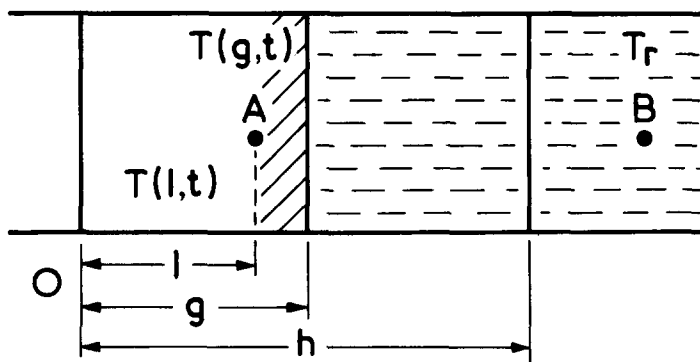


Fig. 7. One-dimensional semi-infinite diffusion model of the temperature measuring system: l , pathlength from O to A in air (0.40 cm); g is the pathlength from O to the working electrode surface (0.05 cm); h is the pathlength from O to the solution (0.10 cm).

right, there are thus 11 boundaries, the working electrode surface being at the sixth. When time $t < 0$, the temperature at all boundaries was set to T_r . When $t = 0$, a constant heat was added to the sixth boundary, so that the temperature change at this boundary was $\Delta T = T(g, 0) - T_r = 1.00 \times 10^{-3} \text{ }^\circ\text{C}$, which was set to 100 units of signal. When $t > 0$, the heat begins to diffuse to both sides at a rate which depends on time and distance from the electrode position and which follows the second-order differential equation

$$\partial T(x, t)/\partial t = \alpha \partial^2 T(x, t)/\partial x^2 \quad (3)$$

The boundary conditions are as described above. According to the numerical differentiation method, the partial differential equation at each boundary can be represented as follows, where $b_1 = \alpha_1 h^2$, $b_2 = \alpha_2 h^2$, $b_3 = \alpha_3 h^2$, h is interval length in the x direction, and α_1 , α_2 and α_3 are the thermal diffusivities of Pt, aqueous solution, and air respectively

$$\begin{aligned} \partial T_1/\partial t &= b_3(T_2 - T_1) \\ \partial T_2/\partial t &= b_3(T_1 - 2T_2 + T_3) \\ \partial T_3/\partial t &= b_3(T_2 - 2T_3 + T_4) \\ \partial T_4/\partial t &= b_3(T_3 - 2T_4 + T_5) \\ \partial T_5/\partial t &= b_1(T_6 - T_5) - b_3(T_5 - T_4) \\ \partial T_6/\partial t &= b_1(T_6 - T_5) - b_2(T_7 - T_6) \\ \partial T_7/\partial t &= b_2(T_6 - 2T_7 + T_8) \\ \partial T_8/\partial t &= b_2(T_7 - 2T_8 + T_9) \\ \partial T_9/\partial t &= b_2(T_8 - 2T_9 + T_{10}) \\ \partial T_{10}/\partial t &= b_2(T_9 - 2T_{10} + T_{11}) \\ \partial T_{11}/\partial t &= b_2(T_{10} - T_{11}) \end{aligned} \quad (4)$$

Based on the SYS-RKN [15] program for solving a partial differential equation, the numerical solution to the above partial differential equations is shown in Fig. 8. When $t = 0$, the temperature change, $\Delta T = T(x, t) - T_r$, is zero at both sides of the working electrode referenced to the reference thermistor, while the ΔT at the electrode surface is 100 units of signal. After 0.005 s, ΔT at the electrode surface begins to decrease, but ΔT at 1.0×10^{-2} cm from the working electrode surface at the air–platinum boundary (where the working thermistor was set up) goes up, while ΔT at the solution side remains zero. This means that the heat diffuses to the working thermistor in 0.005 s; 0.5 s later, the heat flow is passing the thermistor and diffuses into the air, and at the same time ΔT at the solution side begins to go up. After 10 s, the heat flow passes through the zeroth boundary, and heat loss from the Pt slice to the air occurs. This result shows that the thermistor can respond to the temperature change very rapidly because of the good heat conductance of platinum as compared to that of the solution; the temperature loss mostly happens at the Pt slice side, which is responsible for the decrease of E_{OB}/mV with a sweep rate of less than 0.020 V s^{-1} . It also shows that the

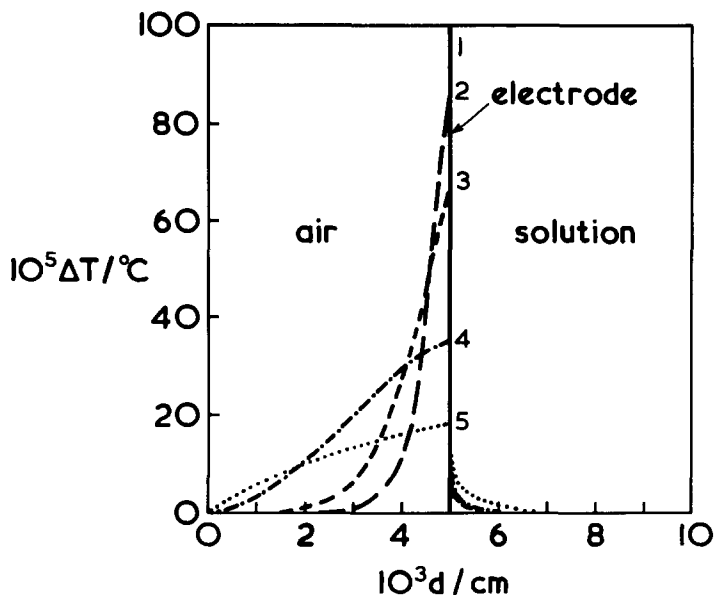


Fig. 8. Calculated temperature change as a function of distance from an infinitely thin electrode surface at different times after raising the temperature of the electrode surface by $1 \times 10^{-3} \text{ }^\circ\text{C}$. Key: 1, $t = 0 \text{ s}$; 2, $t = 0.50 \text{ s}$; 3, $t = 2.0 \text{ s}$; 4, $t = 10.0 \text{ s}$; 5, $t = 40.0 \text{ s}$.

assumption that the temperature at the reference thermistor, T_r , is constant during the experimental time scale in the isothermal cell is correct.

4.2. The concentration distribution and temperature profile in solution

The reaction rate of a simple electrochemical reaction depends not only on the electrochemical reaction rate constant k but also on the sweep rate [16]. If the reaction follows a first-order reaction process, the reaction rate r can be expressed as

$$r = -dc/dt = ke^{-(RT/nF)vt}c^0 \quad (5)$$

where c^0 is the initial concentration of initial substance. In the one-dimensional semi-infinite diffusion model (Fig. 7), we divide the solution side into 10 divisions with increments of $1.00 \times 10^{-4} \text{ cm}$ and 11 boundaries. The zero point is at the working electrode surface. When $t = 0$, the concentration at each division is c^0 , and the potential scans to the point which is just before E^0 . When $t > 0$, the electrochemical reaction takes place with the scan of potential, and c changes with time and position. In our system, $c^0 = 1.00 \times 10^{-3} \text{ mol dm}^{-3}$, the electrode surface area is 1 cm^2 , and 0.20 V overpotential is scanned. During the reaction, the diffusion of initial substance from bulk solution to electrode surface and the diffusion of the substance produced from the electrode surface to the solution are both considered to follow the second law of diffusion

$$\partial^2 c / \partial t^2 = D \partial^2 c / \partial x^2 \quad (6)$$

According to a numerical method [15], the partial differential equation at each boundary can be described as follows

$$D_1 = \partial c_1 / \partial t = -k e^{-(RT/nF)vt} c^0 + D(c_2 - c_1) - D((1 - c_1) - (1 - c_2))$$

$$D_i = \partial c_i / \partial t = D(c_{i+1} - 2c_i + c_{i-1}) - D((1 - c_{i+1}) - 2(1 - c_i) + (1 - c_{i-1})),$$

$$i = 2, 3, \dots, 10 \quad (7)$$

$$D_{11} = \partial c_{11} / \partial t = D(c_{11} - c_{10}) - D((1 - c_{10}) - (1 - c_{11}))$$

where 1, 2, 10, 11, and i indicate terms at the i th boundary, and $D_{\text{reactant}} = D_{\text{product}} = D = 5.0 \times 10^{-6} \text{ cm}^2 \text{ s}^{-1}$. When $k = 0.066 \text{ cm s}^{-1}$ [16], different sets of data have been obtained with different sweep rates. By plotting concentration against distance (d) from the electrode surface, the distribution of concentration with sweep rate was found to be as shown in Fig. 9, from which it can be seen that the range of d is increased with decrease in the sweep rate. Within the reaction layer, the initial molecules have been reduced to the product. By numerically integrating the upper area of each curve, the volume of the reaction layer was obtained, from which the amount of initial substance taking part in the electrochemical reaction could be calculated. The plot of the amount of product against sweep rate (Fig. 10) indicates that, at the same concentration, the current in a cyclic voltammogram increases with sweep rate; however,

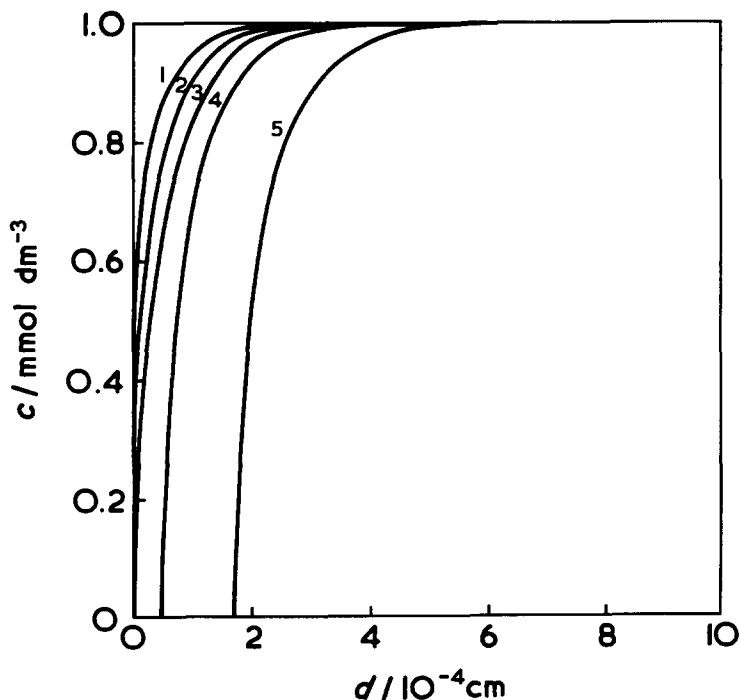


Fig. 9. Distribution of concentration during an electrochemical reaction in the isothermal cell: $c^0 = 1.00 \times 10^{-3} \text{ mol dm}^{-3}$; $D = 5.0 \times 10^{-2} \text{ cm}^2 \text{ s}^{-1}$; $k = 0.066 \text{ cm s}^{-1}$; the area of the electrode surface is 1.0 cm^2 ; sweep rate $v/\text{V s}^{-1}$: 1, 0.10; 2, 0.05; 3, 0.03; 4, 0.02; 5, 0.01.

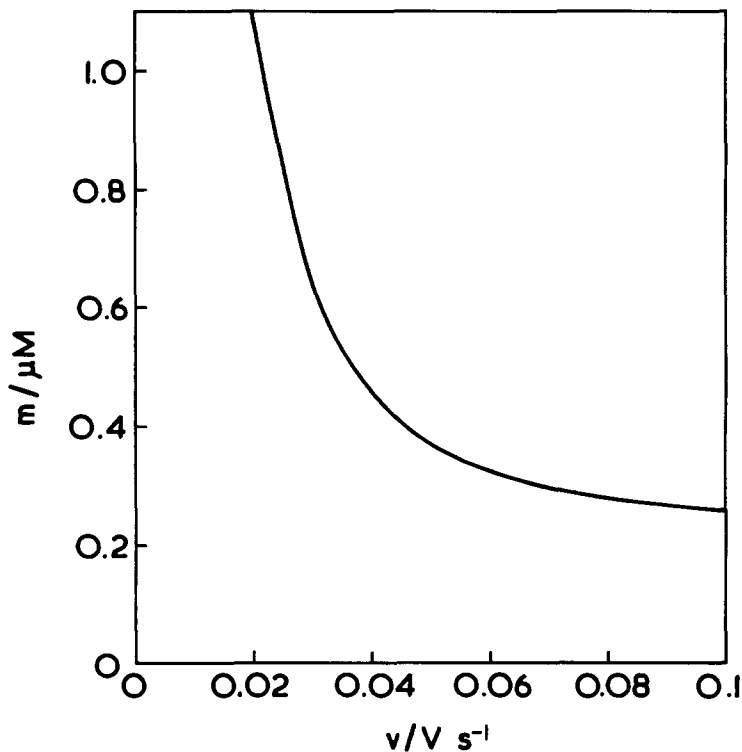


Fig. 10. Plot of the amount of product against sweep rate.

the amount of substance taking part in the reaction decreases with increasing sweep rate (Fig. 10) in the same way as does E_{OB} (Fig. 6, Part II). Since the enthalpy change of the reaction is proportional to the amount of reactant taking part in the reaction, we can conclude that the decrease in the measured temperature with sweep rate (Fig. 6) is due to a decrease in the amount of substance taking part in the reaction.

5. Conclusions

As outlined above, the newly designed electrochemical microcalorimeter shows the following characteristics.

(1) The working thermistor in contact with the working electrode surface provides a fast-response probe for measuring the temperature change during an electrochemical process.

(2) The microcalorimeter can follow a cyclic voltammetric programme, from which the CVT can be used to estimate the enthalpy change of an electrochemical reaction.

(3) From the response function of the calorimeter to sweep rate and from the mathematical treatment, we can see that 0.020 V s^{-1} sweep rate is optimal; at a rate

lower than this, the measured temperature change is reduced by the loss of heat by diffusion from the platinum slice to air; at a rate higher than this, the measured temperature change is decreased due to the reduction of the amount of substance taking part in the electrochemical reaction.

(4) A lock-in amplifier simplifies the Wheatstone bridge circuit, and offers a high-quality amplification of the weak electric signal.

(5) Chemical calibration provides an instantaneously measurable sensitivity factor for the enthalpy of the chemical reaction at the working electrode surface.

Acknowledgements

We thank Professor David E. Williams, Dr D.G. Humphrey, Mr R.D.B. Waymark and Mrs S.A. Gardiner for useful discussions and the SBFSS (Sino-British Friendship Scholarship Scheme) for financial support. Y. Zhu thanks the Shenyang Medical College, China, for leave of absence.

References

- [1] H. Hohne, *Calorimetry—Fundamentals and Practice*, Verlag Chemie, Weinheim, 1984.
- [2] A.T. Kuhn, in A.T. Kuhn (Ed.), *Techniques in Electrochemistry, Corrosion and Metal Finishing*, Wiley, New York, 1987, pp. 291–314.
- [3] V.P. Kolesov, *Pure Appl. Chem.*, 64 (1992) 9–16.
- [4] M. Yamamura, B.N. El, T. Ohkubo, Y. Ishihara, J. Takano, N. Matsunami, K. Kinoshita, T. Miyake, I. Ohtani, Y. Yamaki and M. Yamamoto, *Pure Appl. Chem.*, 65 (1993) 1973–1977.
- [5] G. Olofsson, I. Wadsö and L. Ebersson, *J. Chem. Thermodyn.*, 23 (1991) 95–104.
- [6] G.M. Miskelly, M.J. Heben, A. Kumar, R.M. Penner, M.J. Sailor and N.S. Lewis, *Science*, 246 (1989) 793–796.
- [7] D.E. Williams, D.J.S. Findlay, D.H. Craston, M.R. Sene, M. Bailey, S. Croft, B.W. Hooton, C.P. Jones, A.R.J. Kucernak, J.A. Mason and R.I. Taylor, *Nature*, 342 (1989) 375–384.
- [8] J.M. Sherfey and A. Brenner, *J. Electrochem. Soc.*, 105 (1958) 665–672.
- [9] B.B. Graves, *Anal. Chem.*, 44 (1972) 993–1002.
- [10] K.S.V. Santhanam, N. Jespersen and A.J. Bard, *J. Am. Chem. Soc.*, 99 (1977) 274–276.
- [11] J.R. Smith, P.L. Zanonato and G.R. Choppin, *J. Chem. Thermodyn.*, 24 (1992) 99–106.
- [12] E.J. Prosen and M.V. Kilday, *J. Res. Nat. Bur. Stand.*, 77 (1973) 581–597.
- [13] B.W. Kenneth and R.S. Robert, *J. Chem. Thermodyn.*, 11 (1979) 773–786.
- [14] Y. Zhu and R.J.H. Clark, to be published.
- [14a] Y. Zhu, in preparation.
- [15] K. Ebert, H. Ederer and T.L. Isenhour, *Computer Applications in Chemistry—An Introduction for PC Users*, VCH Publishers, New York, 1989, p. 312.
- [16] J. Koryta, J. Dvorak and L. Kavan, *Principles of Electrochemistry*, 2nd edn., Wiley, New York, 1993, p. 258.